Webology (ISSN: 1735-188X)
Volume 18, Number 4, 2021

COVID-19 Detection And IP Discrimination Using Deep Learning – State Of The Art

Ume Hani , Muhammad Naeem , Asim Shahzad, Muhammad Zeeshan , Muhammad Imran Khan , Muhammad Zubair Tahir , Muhammad Sibt ul Hassan , Muhammad Asshad , Aamir Khan

Abbottabad University of Science and Technology, Abbottabad, KPK, Pakistan.

Abstract. Due to its high usage, the diagnostic availability for SARS-COV-2 and Influenza pneumonia (IP) is Reverse Transcription Polymerase Chain Reaction (RT-PCR). IP of types A and B with more different sub-types contains similar biological features related to the SARS-COV-2. Due to SARS-COV-2variations, the medical results may not differentiate the novel SARS-COV-2 and many forms of IP. Real-Time transcriptase Polymerase Chain Reaction (RT-PCR) is used to detect SARS-COV-2 but possesses a high negative false rate. Early and accurate detection of SARS-COV and IP demands a medical specialist's assistance to treat and recover patients from diseases according to its modality. Accurate detection of SARS-COV-2 and IP is challenging for medical experts due to the same mode of diseases and unavailability of high positive rate tests. Our objective of the research is to review the SARS-COV-2 detection techniques so that in the future, DL model-based discrimination with other pneumonia will be achieved with highly accurate results.

Keywords: COVID-19, SARS-COV-2, RT-PCR.

1 Introduction

Severe Acute Respiratory Syndrome Coronavirus (SARS-COV-2) is a respiratory disease, a type of COVID-19 spread worldwide and causes the pandemic. Coronavirus possesses many forms in the human body as well as in animals. Human coronavirus (Hcov) further split into mild and severe coronavirus. SARS-COV-2 is life-threatening, having effects on respiratory cells, bronchial epithelial, and pneumocystis. Replicating SARS-COV-2 active particles in the body and person-to-person transmission causes a more alarming situation [1]. High-intensity SARS-COV-2 may result in any organ failure such as acute kidney and lungs disorder. The source of respiratory disease is influenza pneumonia, which may lead to critical health issues. SARS-COV-2 and IP are respiratory diseases having similar modes of transmission. These respiratory diseases seem to be more complicated with high death rates. The spread rate of SARS-COV is so high that it spreads throughout the world in a very minimum time. The virus attacks human bodies through saliva discharge from the nose during sneezes or cough. Affected people may experience fever, cough, headaches, chest pain, and loss of taste and smell. SARS-COV becomes more complicated day-by-day having its non-identical impact on the human body in different phases. Investigation and analysis for the detection of SARS-COV is the most demanding proposal of the time. Deep learning algorithms produced efficient results on medical image analysis and provided a high positive rate [2]. In this paper, we will evaluate the different state of the art deep learning approaches for the precise improved detection of COVID-19 lesions.

1.1 X-Ray and CT Image Dataset

X-ray dataset categorized into four classes of bacterial, normal, viral, and COVID. Kaggle dataset used for the viral, normal, and bacterial set. COVID dataset was collected from two sources of 1000 image repositories of the Italian Society of Medical & Interventional Radiology and Radiopaedia [1]. Mendeley dataset is used for the other 900 images. For generating an augmented dataset, random rotation, random horizontal/vertical shear, and random horizontal/vertical reflection are employed for the experimentation 80% dataset used for training and 20% for the testing process. For requirement completion of deep models, dataset images are resized to 224 by 224 for MobileNetV2 and 299 by 299 for Inception3. Dataset X-ray images are cropped for the removal of noise to enhance the quality of images. During experimentation, it is observed that limited datasets produce better results on conventional shallow CNN models. [2] the objective was to produce synthetic images to overcome the overfitting problem. Kaggle dataset of 145 posteroanterior chest datasets of COVID-19 CXR was used. Synthetic and non-synthetic images performance ver different model is also compared. Dataset fractionates into synthetic 130 and non-synthetic 145 COVID, bacterial pneumonia along with normal patients images.

High-quality CXR for COVID-19 class fine-tuning is performed by adopting GAN architecture. The entire dataset is recreated using pre-processing techniques producing masked images. To reduce the anatomical structure black rectangle shape is used. [3] collected dataset from Indore and Maharashtra sectors from India. The dataset contains X-ray images of posteroanterior (PA) fore chest visibility. Dataset categorized 2into X-rays of COVID, normal and viral infected people. For image enhancement preprocessing step comprises of cropping images by Masked-R-CNN. Annotations of the images and detection of X-ray images YOLO model employed. To get maximum information, images are stored in RGB format. [4] dataset contains chest images of anterior-posterior pneumonia X-ray. Dataset categorized into viral, bacterial pneumonia, healthy and COVID affected samples. Visually discrimination between dataset samples is not recognizable. Data is normalized between zero and one due to distinct repositories data. Images are resized 224 by 224 for decreasing the computational time. GAN network is used to remove overfitting problems. [5] obtained 1001 CX images from the open public with labelling process done by radiologist and specialist. Sobel, Robert, and Prewitt gradient operators are computed. Watershed ridge line and catchment basins on images achieved by watershed transformation using the below mathematical computation

$$CB(m_j) =\{ x \in S \mid \nabla i \in F \{i\} : g(m_j)+T_f(x,m_j)< g(m_i) + T_f (x,m_i)\} \ldots\ldots\ldots \; (1)$$

Functioning $g \in CS$, for F a minimum mk Where $K \in F$, set of point (x) with minima mj of catchment basin CB (mj) closer to mj topographically than local minima mi. Domain and topographical distances are S and Tf. MCWS algorithm is used to separate small and large details in X-ray images. [6] used dataset from two sources named COVID-Chest-X-ray by Cohen JP and Normal Chest X-ray collected from GitHub repository of 500 images. For stability in CNN architecture, X-ray images are normalized in the range 0 to 1. Dataset images are grayscale, so rescaling is executed through multiplying pixel by 1/255. Dataset images for the training model are in low quantity, so to overcome this problem, data augmentation is applied with a four-step process keeping class labels while enlarging data images. [7] used QaTa-COV19 dataset due to its versatility. QaTa-COVID19 dataset contains 6,200 images collected from different countries. After the normalization process with unit variance and zero mean feature vector are obtained. For query samples, PCA is applied for dimensionality reduction.

MOSMED and CCAP databases are used for the COVID-19 lesion detection [8]. Dataset comprises of 3D CT scan having 40 axial slices of each CT scan. The first and last slice of lung CT scan is denoted by one, and T. Number of images I 3D CT volume is shown by T. Middle axial lung slice is determined by dividing T by 2. CCAP dataset includes healthy, COVID-19, bacterial, viral, mycoplasma and pneumonia infected images. In preprocessing step, data augmentation is performed. High performance can be achieved by utilizing high-speed memory. [9] uses Zhao and Xie dataset that claimed to be the most essential COVID-19 CT scan image data. Seven hundred sixty preprints were collected from bioRxiv3 and medRxiv2. Python package is used for the extraction of CT images from preprints. 349 CT images of positive COVID-19 selected with different image sizes. In preprocessing, images are resized 224 x 224. Data augmentation I applied with random affine transformation with normalization. Due to the small size, the dataset deep learning model resulted in a low accuracy rate and facing an overfitting problem.

[10] the dataset is based on Wuhan University Renmin Hospital and two affiliated hospitals. CT scans of 88 COVID-19 infected images are collected. Covid infected people were evaluated after RT-PCR. Moreover, 86 healthy, and 100 bacterial pneumonia was taken for deep learning. In preprocessing, lung segmentation is achieved after image contouring to avoid noise from CT images. In the study, limited dataset usage resulted in an overfitting problem. [11] uses a publicly available dataset of 15,589 CT images with 95 COVID positives and 48,260 COVID negative people. 16-bit tiff format images are resized to 512 x 512. No preprocessing is applied to the dataset images for noise removal. [12] Two hundred ninety-three patients were involved in the experiment, and 371 CT scans were collected from Beijing Haidian Hospital. 98 COVID-19, 157 other CAP patients along with 38 viral influenzas having 27% mild, 2.3 severe, and 0.8 critical. Evaluation of annotation performance with dice index was measured as follows

$$DiceLoss = 1 - \frac{2 \times Predicted \times Annotation}{Predicted + Annotation}$$

[13] uses Mosmed dataset as mentioned in Figure 1. To attain isotropic resolution whole dataset was resampled. Segmentation was used to gain model reliability. Hounsfield unit used to calculate mask on CT images. Segmented regions resulted in a non-informative portion. To eliminate unrelated regions with no information, image CT scans were cropped. [14] the dataset comprises 201 patients from China. CT image of 512 x 512 down sampled to 256 to 256. In preprocessing, the histogram is used to gain greater image frequency with the spatial field concept. [15] uses 2482 CT image datasets of 1252 CT images with SARS-COV-2 and 1230 CT images with normal people. In preprocessing process same size and intensity are produced by reducing dimensions to 120 x 120 x 3. For edge detection filter with values {0,-1,0},{-1,6,-1} and {0,-1,0}was applied. RGB images converted to YUV for luminance. At

last, YUV converted back to RGB for equalizing intensity values with histogram equalization and smoothing edges.

2 Deep Leaning based Feature Extraction and Segmentation

Unbalanced and inadequate X-Ray or CT images should be analyzed for deep detection of COVID-19 [16]. To train a deep architecture dataset, images are substandard, so it is more appropriate to use a hand-crafted feature extraction method for analyzing images. GLCM, LBGLCM, GLRLM, and SFTA extract features from 260 images increased after image augmentation from 126 to 260.

Feature vectors are combined using four techniques resulted in 78 features from each image. SMOTE method is used for oversampling 78 features of 260 images and trained on PCA and SAE architecture. The advantage of using SAE and PCA is to shrunken features from 78 to 20. For classification, SVM is trained on 495 vectors having 20 shrunken features. Pulmonary, patchy ground-glass, and reticulonodular opacities are the non-identical radiographic patterns in COVID-19 patients [17]. Radiomic textures are used to exhibit visual character representations. Eight FOSF (First Order Statistical Features), HOG 8100, and GLCM utilize 88 features. A complete description of the image was obtained using kurtosis energy, entropy, mean, and variance. Local neighborhood information does not scrutinize by global texture patterns. Analysis of in-depth texture used to get high performance of GLCM and HOG. Local shape or textural information encoded by HOG features and four discrete directions 00, 450, 900,1350 of spatial correlation between pixel intensities carried out by GLCM.

Table 1 Number of Features Extracted

Algorithm	Offset Parameters	Feature Extracted per Image
GLCM	[2 0]	22
LBGLCM	[2 0]	22
GLRLM		7
SFTA	5	27

In the natural medical pattern of textural images are effectively encoded by statistical features. Each CXR image obtained 8196 features using FOSF, GLCM, and HOG. Extracted features are not visually accurate resemble COVID-19 features. To extract the most relevant features BGWO (Binary Grey Wolf Optimization) is used. To upgrade the models of the deep learning feature extraction method, PCA is employed [18]. Image scaling and normalization are done in preprocessing step because of different image dimensions in height and width. For orthogonal transformation, images are inputted into PCA to extract predominant features associated with variance 1. Studies have shown that the machine learning model achieves high results with feature extraction methods in the initial steps. Features extracted from X-Ray or CT images are concatenation possess the advantage to combine distinct image features [19]. For Region of Interest, images are inputted through the process of image segmentation. Features are extracted from X-Ray and CT images with two different methods. Initially, features are extracted from CT and X-Ray through CNN, and afterward, extraction of features is done by CNN GoogleNet and ResNet-18. DFC concatenates different features so that the classification process is upgraded and innovated into high accurate results.

Due to high positive results in the concatenation of features fusion approach with two process are introduced. RGB images converted into greyscale and computed ROI [20]. In the first stance of the feature extraction method, HOG is used with CNN.

HOG extracts feature from greyscale images, then the same images used for feature extraction through CNN, and then 7876 extracted features from HOG and CNN inputted to classification model for training. For the identification of COVID-19 large numbers of features are required for precise recognition. The difficulty may arise for the feature set on a small dataset. Generalization of feature set on small dataset lead to high complications [21]. To overcome minor database issues, VGG16 truncated architecture is proposed with initial four blocks of convolution. For overfitting, PCA is used for the image feature selector. GLCM shows the adjacency between two pixels of the image with size and angle [22]. Textural feature using GLCM features correlation, homogeneity, energy, and contrast. Statistical feature kurtosis, standard deviation, and skewness are employed. Prelearned deep feature extractor CNN-based AlexNet architecture proposed for classification [23].

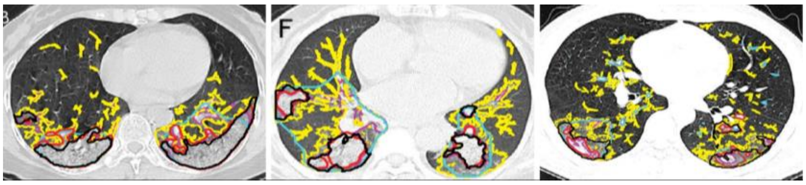

Figure 1 a) Segmented lesion mask detection b) Segmentation result of COVID-19 [29]

The advantage of the model trained over 1 million images gives rise to good performance. Relief algorithm used for feature selection established on KNN algorithm. Prelearned AlexNet shows 97.21 accuracies for the Conv5 layer. Selected features using Relief algorithm with 100 step size tuned to 2005000 range and performance evaluated by SVM. The study showed the limitation of the optimal values for the Relief algorithm that may affect classification results. Quantification and diagnosis of diseases through medical imaging segmentation are helpful. Minor regions of interest in the medical images (X-Ray or CT) are extracted using segmentation, and targeted lesions are quickly evaluated. [24] Proposed FSS model trained on CT axial scan of number N with annotation map for each semantic label. Unit of measurements of number three for FSS is the path of conditioner, adaptive interaction, and segmentation path. From a slice of visual query statistics learned in the conditioner path. Learned feature map representations pass to segmentation path from adaptive interaction. In the segmentation path, every slice of a query is segmented and obtained appropriate representations. On the feature map, scaling of cross channel features is carried out in the segmentation path. Conv 1x1 layer block brings out segmentation maps in classification. Segmentation maps assigned to Softmax function for the speculation of targeted lesions in each image slice. Encoder-Decoder Deep neural network model for deep segmentation SegNet used to reduce complexities encountered in the segmentation process [25]. The encoder layer for segmentation is similar to VGG16, and the decoder layer uses max-pooling indices for the segmentation mask.

Table 2. Comparative Analysis of Segmentation Techniques

Author	Database	Methodology	Results	Limitation
Basset et al	Italian Society of Medical and Interventional Radiology	FSS	Dsc = 0.798	Improved parameters should be used for uncertainty

				and complex prediction to gain high improved results
Saood et al	Italian Society of Medical and Interventional Radiology	SegNet	Acc = 0.97	Results can be enhanced by generalizing detailed training and testing experiments
Wu et al	438 Paitents from 2 Chinese Hospital	SRGNET	Acc = 83.2	Results dependent on the interpretation of medical experts turned into a time consuming task. SRGNET doesn't discriminate COVID-19 with other pneumonia diseases.
Zhao et al	Lungs CT	D2D U-Net	Dc = 0.7298 Pixel Error = 0.0311	For the high rate performance of D2D U-Net model parameters

				and used channel numbers should be reduce so that the decoder parameters may not exceed to large parameters
Oulefki et al	EL-BAYANE	GraphCut, Watershed, MIS	Acc = 0.98	Manual segmentation can be improved for better results. Other viral pneumonia discrimination is not possible with proposed approach
Chen Zhao et al	112 CT Scan from Shanghai Public Health Clinical Centre	SP-V-Net	Acc = 0.97	Improvement can be done through active contours shape priors
Zhou et al	Italian Society of Medical and Interventional Radiology	U-Net	Dc = 83	Large dataset can be applied for the refinement of the training process

Hyperparameters for training SegNet with ILR Ie-4, Ie-3, and 3e-3 with MiniBatch 4,8,12 of nine experiments executed. In experiment four, binary segmentation attained an accuracy of 0.95, and multi-class segmentation best result was carried out in experiment seven. COVID-19 lesions detection by 2D patch-based SRGNET (Sequential Supervised Segmentation) is supervised segmentation accommodating productivity of predictions in multiscale segmentation [26]. Tensor flow GPU 1.8.0 was used for the implementation of the proposed SRGNET. Unbalancing problem and cost of computation not encountered due to boundary boxes generation in different network layers. The process of post-processing enhances the results of segmentation with local and global features. U-Net-based image segmentation architecture is encoder-decoder-based architecture in which the encoder achieves downsampling from max-pooling and convolutional layers [27]. Transposed convolution is used for the precise localization for up-sampling. This process is desirable for the analysis of images at the pixel level. Prediction of output mask has resulted from ground truth mask of input the input image. Performance evaluation for the segmentation model is executed with a loss function. The segmentation process may accommodate blur edge and irregular pattern challenges [28].

To overcome these problems, dilated dual attention D2D U-Net was introduced for segmenting the COVID-19 lesions. The model is built on hybrid dilated convolutions and a dual attention approach. D2D U-Net model GAM (Gate Attention Module) and DAM (Decoder Attention Module) were employed to diminish semantic gap and feature clarification. To improve the bound interrelation in the network signals of the semantic gate and feature fusing implemented in GAM. For the high quality of segmentation of COVID-19 lesion, DAM is adopted as a decoder model to enhance the decoding quality. Dilated hybrid convolution is manipulated for regular segmentation and high receptive range. ImageNet-1K utilized for the pretraining with 32x4d ResNeXt-50 encoder. Connection full layers and average global pooling eradicated from the network.

Output channel 64-256-512-1024-2048 is used as in the actual ResNeXt model accommodates. [29] GraphCut, Watershed, and MIS (Medical Image Segmentation) techniques for the image enhancement with segmentation showed superior, efficient results. COVID-19 lesions present at borders are non-detectable using the Watershed technique. For the discrimination between the lesions of the COVID-19 features set, the colormap is used to split CVOID lesions into red, blue, and green to interpret the severity level. 3D-V-Net with shape deformation was used to extract each portion of lungs for initial knowledge [30]. For pulmonary parenchyma, the binary thresholding technique is applied on the CT images with a -320 threshold. The volume of the CT scan is evaluated for eliminating discrete regions with less than 1% volume region is abolished, and greater than 1% region is reserved. Boundaries of the evaluated regions are smoothened by morphological closing operation. Substandard image quality resulted in low-quality results, leading to the poor evaluation of the infected regions of the targeted problem [31]. Two-step processes of the transfer learning approaches are used for upgrading the image quality with segmentation. In an initial step, images are trained on chest radiograph, and in the second step, refine knowledge from chest images obtained having the dangerous pandemic condition. During the training phase, changes in gradient cause the features degradation learned previously in the pretraining phase. The network is extended to the domain translator module by adding new layers and the original layer by weight freezing. Unsupervised image segmentation performed using the operation of morphological reconstruction resulted in the removal of irregularities on lesion areas [32]. Contrast matrix of edge content used for the structural element of optimal size. Noise removal is performed by morphological reconstruction.

Encoder-Decoder architecture with skip connections named U-Net was adopted for the effective segmentation [33]. Max pooling, activation of ReLu, and convolution of different layers involved in the encoder. The deconvolution process induces the segmentation mask. The utilization of skip connections helps to collect minor information from a high-resolution dataset. [34] 0.29 seconds for the image segmentation on each CT slice is encountered using encoder-decoder U-Net architecture 3x3 convolution of stride 2 with number raise from 32 to 512. Focal Tversky loss adapted for the training purpose of the model which increases the ROI segmentation.

2 Conclusion and Future Work

High transmissibility and variations in COVID-19 are challenging for medical experts to diagnose with precise results. False-negative results are experienced in the detection of COVID-19 using RT-PCR, serology, and radiology examination test. Compilation of various DL approaches in the paper showed better results than manual testing processes. Due to limited training data, DL techniques interpretation affects results as compared to large datasets. In the future, we will develop a novel DL model for the error-free detection of distinct coronavirus disease on large-scale training data to upgrade medical imaging results.

Acknowledgments. The heading should be treated as a 3rd level heading and should not be assigned a number.

References

1. Ahmad, F., Khan, M. U. G., & Javed, K. (2021). Deep learning model for distinguishing novel coronavirus from other chest related infections in X-ray images. Computers in biology and medicine, 134, 104401.
2. Karakanis, S., & Leontidis, G. (2021). Lightweight deep learning models for detecting COVID-19 from chest X-ray images. Computers in biology and medicine, 130, 104181.
3. Nigam, B., Nigam, A., Jain, R., Dodia, S., Arora, N., & Annappa, B. (2021). COVID-19: Automatic detection from X-ray images by utilizing deep learning methods. Expert Systems with Applications, 176, 114883.
4. Sheykhivand, S., Mousavi, Z., Mojtahedi, S., Rezaii, T. Y., Farzamnia, A., Meshgini, S., & Saad, I. (2021). Developing an efficient deep neural network for automatic detection of COVID-19 using chest X-ray images. Alexandria Engineering Journal, 60(3), 2885-2903.
5. Demir, F. (2021). DeepCoroNet: A deep LSTM approach for automated detection of COVID-19 cases from chest X-ray images. Applied Soft Computing, 103, 107160.
6. Nayak, S. R., Nayak, D. R., Sinha, U., Arora, V., & Pachori, R. B. (2021). Application of deep learning techniques for detection of COVID-19 cases using chest X-ray images: A comprehensive study. Biomedical Signal Processing and Control, 64, 102365.
7. Yamaç, M., Ahishali, M., Degerli, A., Kiranyaz, S., Chowdhury, M. E., & Gabbouj, M. (2021). Convolutional Sparse Support Estimator-Based COVID-19 Recognition From X-Ray Images. IEEE Transactions on Neural Networks and Learning Systems, 32(5), 1810-1820.
8. Saha, P., Sadi, M. S., & Islam, M. M. (2021). EMCNet: Automated COVID-19 diagnosis from X-ray images using convolutional neural network and ensemble of machine learning classifiers. Informatics in medicine unlocked, 22, 100505.
9. Serte, S., & Demirel, H. (2021). Deep learning for diagnosis of COVID-19 using 3D CT scans. Computers in biology and medicine, 132, 104306.

10. Li, C., Yang, Y., Liang, H., & Wu, B. (2021). Transfer learning for establishment of recognition of COVID-19 on CT imaging using small-sized training datasets. Knowledge-Based Systems, 218, 106849.
11. Y. Song et al., "Deep learning Enables Accurate Diagnosis of Novel Coronavirus (COVID-19) with CT images," in IEEE/ACM Transactions on Computational Biology and Bioinformatics, doi: 10.1109/TCBB.2021.3065361.
12. Mohammadpoor, M. (2021). A deep learning algorithm to detect coronavirus (COVID-19) disease using CT images. PeerJ Computer Science, 7, e345.
13. Zhang, X., Wang, D., Shao, J., Tian, S., Tan, W., Ma, Y., ... & Zhang, Z. (2021). A deep learning integrated radiomics model for identification of coronavirus disease 2019 using computed tomography. Scientific reports, 11(1), 1-12.
14. Rohila, V. S., Gupta, N., Kaul, A., & Sharma, D. K. (2021). Deep learning assisted COVID-19 detection using full CT-scans. Internet of Things, 14, 100377.
15. Castiglione, A., Vijayakumar, P., Nappi, M., Sadiq, S., & Umer, M. (2021). COVID-19: Automatic Detection of the Novel Coronavirus Disease from CT Images Using an Optimized Convolutional Neural Network. IEEE Transactions on Industrial Informatics.
16. Öztürk, Ş., Özkaya, U., & Barstuğan, M. (2021). Classification of Coronavirus (COVID-19) from X-ray and CT images using shrunken features. International Journal of Imaging Systems and Technology, 31(1), 5-15.
17. Chandra, T. B., Verma, K., Singh, B. K., Jain, D., & Netam, S. S. (2021). Coronavirus disease (COVID-19) detection in chest X-ray images using majority voting based classifier ensemble. Expert systems with applications, 165, 113909.
18. Rasheed, J., Hameed, A. A., Djeddi, C., Jamil, A., & Al-Turjman, F. (2021). A machine learning-based framework for diagnosis of COVID-19 from chest X-ray images. Interdisciplinary Sciences: Computational Life Sciences, 13(1), 103-117.
19. Saad, W., Shalaby, W. A., Shokair, M., Abd El-Samie, F., Dessouky, M., & Abdellatef, E. (2021). COVID-19 classification using deep feature concatenation technique. Journal of Ambient Intelligence and Humanized Computing, 1-19.
20. Ahsan, M., Based, M., Haider, J., & Kowalski, M. (2021). COVID-19 detection from chest X-ray images using feature fusion and deep learning. Sensors, 21(4), 1480.
21. Singh, M., Bansal, S., Ahuja, S., Dubey, R. K., Panigrahi, B. K., & Dey, N. (2021). Transfer learning–based ensemble support vector machine model for automated COVID-19 detection using lung computerized tomography scan data. Medical & biological engineering & computing, 59(4), 825-839.

22. Osman, A. H., Aljahdali, H. M., Altarrazi, S. M., & Ahmed, A. (2021). SOM-LWL method for identification of COVID-19 on chest X-rays. PloS one, 16(2), e0247176.
23. Turkoglu, M. (2021). COVIDetectioNet: COVID-19 diagnosis system based on X-ray images using features selected from pre-learned deep features ensemble. Applied Intelligence, 51(3), 1213-1226.
24. Abdel-Basset, M., Chang, V., Hawash, H., Chakrabortty, R. K., & Ryan, M. (2021). FSS-2019-nCov: A deep learning architecture for semi-supervised few-shot segmentation of COVID-19 infection. Knowledge-Based Systems, 212, 106647.
25. Saood, A., & Hatem, I. (2021). COVID-19 lung CT image segmentation using deep learning methods: U-Net versus SegNet. BMC Medical Imaging, 21(1), 1-10.
26. Wu, J., Xu, H., Zhang, S., Li, X., Chen, J., Zheng, J., ... & Ji, R. (2021). Joint segmentation and detection of COVID-19 via a sequential region generation network. Pattern recognition, 118, 108006.
27. Hasan, M. J., Alom, M. S., & Ali, M. S. (2021, February). Deep learning based detection and segmentation of COVID-19 & pneumonia on chest X-ray image. In 2021 International Conference on Information and Communication Technology for Sustainable Development (ICICT4SD) (pp. 210-214). IEEE.
28. Zhao, X., Zhang, P., Song, F., Fan, G., Sun, Y., Wang, Y., ... & Zhang, G. (2021). D2A U-Net: Automatic Segmentation of COVID-19 CT Slices Based on Dual Attention and Hybrid Dilated Convolution. Computers in biology and medicine, 104526.
29. Oulefki, A., Agaian, S., Trongtirakul, T., & Laouar, A. K. (2021). Automatic COVID-19 lung infected region segmentation and measurement using CT-scans images. Pattern recognition, 114, 107747.
30. Zhao, C., Xu, Y., He, Z., Tang, J., Zhang, Y., Han, J., ... & Zhou, W. (2021). Lung Segmentation and Automatic Detection of COVID-19 Using Radiomic Features from Chest CT Images. Pattern Recognition, 108071.
31. Vidal, P. L., de Moura, J., Novo, J., & Ortega, M. (2021). Multi-stage transfer learning for lung segmentation using portable X-ray devices for patients with COVID-19. Expert Systems with Applications, 173, 114677.
32. Chakraborty, S., & Mali, K. (2021). A morphology-based radiological image segmentation approach for efficient screening of COVID-19. Biomedical Signal Processing and Control, 69, 102800.

33. Saeedizadeh, N., Minaee, S., Kafieh, R., Yazdani, S., & Sonka, M. (2021). COVID TV-Unet: Segmenting COVID-19 chest CT images using connectivity imposed Unet. Computer Methods and Programs in Biomedicine Update, 1, 100007.
34. Zhou, T., Canu, S., & Ruan, S. An automatic covid-19 ct segmentation network using spatial and channel attention mechanism (2020). arXiv preprint arXiv:2004.06673.